

Experimental and numerical studies of dynamic rupture propagation in a large laboratory rock sample

P.I.: N. M. Beeler, USGS, Menlo Park, California; T. E. Tullis, Brown University, Providence, Rhode Island

Original proposal: *To perform laboratory experiments and numerical simulations of dynamic rupture on a large fault surface capable of producing repeated, confined, dynamic ruptures (Figure 1). Rupture propagation and arrest will be studied on faults with homogeneous material properties and on faults with heterogeneous stress and material properties of known spatial extent. The geophysical purpose of this research is measure directly the energy budget of seismic faulting with known spatial distribution of fault strength, pre-stress, pre-slip and material properties. Direct measurement of the spatial distribution of seismic slip and fracture energy will be available for comparison with values inferred from off-fault but near-field sensors. 3D dynamic rupture simulations of the lab experiments will be conducted using finite difference methods.*

Introduction. Funding from SCEC was used to support 3 months of graduate stipend, living expenses and travel for Terry's graduate student Jenni Junger to work at the USGS Menlo Park Campus from June through August 2004 with Brian Kilgore and Nick Beeler in Jim Dieterich's lab. During that time Jenni, Brian and Nick conducted dynamic rupture experiments on faults with homogeneous and heterogeneous strength. All of these tests were unconfined. The homogeneous faulting experiments provide a baseline for comparison to existent heterogeneous and subsequent experiments. As, during the course of our study, we produce repeated dynamic rupture resulting from constant rate loading, we decided to expand the focus of our study to consider predictability of rupture onset using probabilistic, and precursory approaches.

Results. Homogeneous rupture were conducted on a 2 m long fault surface of Sierra granite at 4 and 2 MPa normal stress and loading rates between 0.0001 and 0.001 MPa/s. Data consist of 0.5s duration, triggered megahertz rate recordings of local stress, slip, and acceleration at a number of locations on the surface of the fault blocks (Figure 2a and 2b), and 100 Hz, long duration records of far-field stress, local stress and local displacement. The fault surface is rough by laboratory standards, having a peak to peak roughness of approximately 80 microns. The high roughness produces a very large nucleation zone (> 0.5 m in length), relatively large and easily detectable precursory slip, relatively large apparent fracture energy, and slow rupture propagation and slip rates. The size of the nucleation zone can be estimated from low speed recordings (Figure 3a) that show strength loss due to slip in the center of the fault during loading (g7,g9) which transfers stress to the fault ends (g14,g13, g2, g3). This large precursory slip in the fault center requires that in the nucleation zone much of the potential strength loss has already occurred prior to the onset of dynamic rupture, as apparent from the high speed record of this event (Figure 3b). Thus dynamic stress drop is very small in the fault center and large at the ends. Similarly, fracture energy is small at the fault center and large at the ends.

A second set of heterogeneous faulting experiments were conducted. To induce interseismic fault creep at one end of the fault and produce stress and strength heterogeneity we added a thin layer of fault gouge to one end of the fault (Figure 4a). Our intention was to both to reduce the

pre-stress and to confine the rupture at that end. However this fault gouge instead made the fault stronger and induced locking at that end, probably due to increased area of contact. The end result was a heterogeneous fault with complex rupture (Figure 4b).

Earthquake prediction. We also considered some preliminary aspects of earthquake prediction using successive events from our homogeneous faulting experiments. The event to event reproducibility of loading time (recurrence interval), failure stress, stress drop, and precursory activity can be interpreted as indications of the intrinsic variability of small earthquake occurrence and source physics in this controlled setting. At 4 MPa normal stress and a loading rate of 0.0001 MPa/s, the loading time is ~25 min., with coefficient of variation of around 10%. Static stress drop has a similar variability which results almost entirely from variability of the final (rather than the initial) stress. The variability of loading time to failure is comparable to the lowest variability of recurrence time of small repeating earthquakes at Parkfield (Nadeau et al., 1998) and our result may be a good estimate of the intrinsic variability of recurrence, presuming that our measurements are not influenced by apparatus effects. Distributions of loading time can be adequately represented by a log-normal or Weibull distribution (Figure 5a) but long term prediction of the next event time based on probabilistic representation of previous occurrence is not dramatically better than for field-observed small- or large-magnitude earthquake datasets.

At constant loading rate, the gradually accelerating precursory aseismic slip observed in the region of nucleation in these experiments is consistent with the observations and theory of Dieterich and Kilgore (1996). Precursory strains can be detected typically after 50% of the total loading time. The Dieterich and Kilgore approach implies an alternative method of earthquake prediction based on comparing real-time strain monitoring with previous precursory strain records or with physically-based models of accelerating slip. Near failure, time to failure t is approximately inversely proportional to precursory slip rate V (Figure 5b). Based on a least squares fit to accelerating slip velocity from ten or more events, the standard deviation of the residual between predicted and observed $\log t$ is typically 0.14. Scaling these results to natural recurrence suggests that a year prior to an earthquake, failure time can be predicted based on measured fault slip rate with a typical error of 140 days, and a day prior to the earthquake with a typical error of 9 hours. However, such predictions require detecting aseismic nucleating strains, which have not yet been found in the field, and on distinguishing earthquake precursors from other strain transients. There is some field evidence of precursory seismic strain for large earthquakes (Bufe and Varnes, 1993) which may be related to our observations. In instances where precursory activity is spatially variable during the inter-seismic period, as in our experiments, distinguishing precursory activity might be best accomplished with deep arrays of near fault instruments and pattern recognition algorithms such as principle component analysis (Rundle et al., 2000).

Plans and completion activities: In 2005 we will complete the laboratory aspects of this study using a smooth fault, leading to small nucleation patch size, high slip and rupture velocity, low fracture energy and relatively large dynamic stress drop. Rather than quartz powder we will use illite clay to produce weak rate strengthening regions that will creep steadily. Data from homogeneous faulting experiments on the smooth fault will be passed to the SCEC dynamic rupture code validation project for consideration. Dynamic rupture modeling of our homogeneous and heterogeneous results will commence in 2005.

We have not requested additional funding for this project from SCEC in 2005. We expect to report our final results at the 2005 SCEC meeting, and continue studying the effects of heterogeneity on rupture propagation and on earthquake occurrence for the next few years.

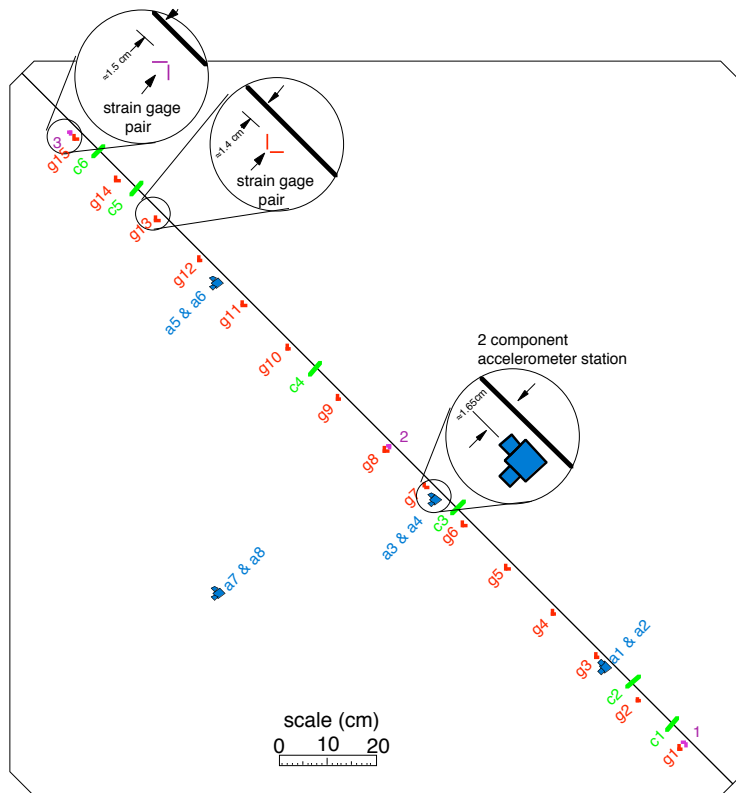
References

Bufe, C.G, and D. J. Varnes, J Predictive modeling of the seismic cycle of the greater San Francisco Bay region, *Journal of Geophysical Research*, 98, 9871-9883, 1993.

Dieterich, J.H., and B. Kilgore, Implications of fault constitutive properties for earthquake prediction, *Proc. Natl. Acad., Sci. USA*, 3787-3794, 1996.

Nadeau, R. M, and L. R. Johnson, Seismological studies at Parkfield VI; moment release rates and estimates of source parameters for small repeating earthquakes, *Bulletin of the Seismological Society of America*, 88, no.3, 790-814 1998.

Figures



instrument locations are approximate on schematic

Key





 upper shear strain gauge	 lower shear strain gauge
 accelerometer station	
 cantilever type slip gauge	

Figure 1. Scaled diagram of Dieterich's large laboratory fault, including instrumentation type and location.

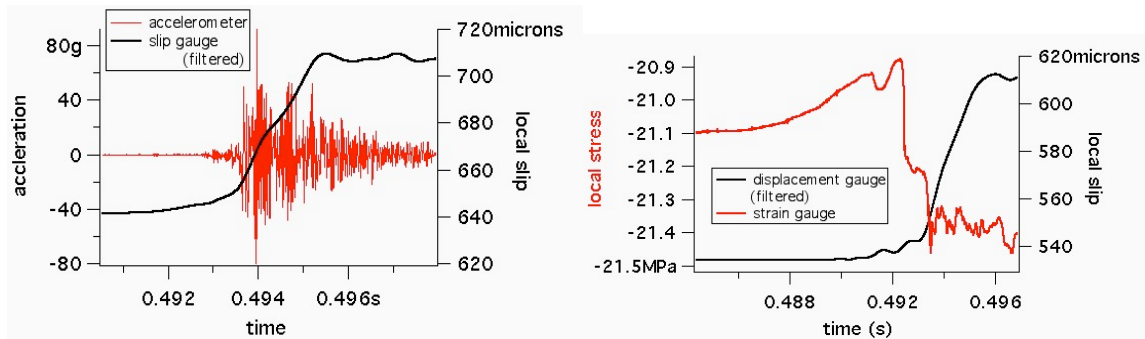


Figure 2. Example high speed recordings of co-located acceleration and slip (a), and stress and slip (b) adjacent to the fault during dynamic rupture.

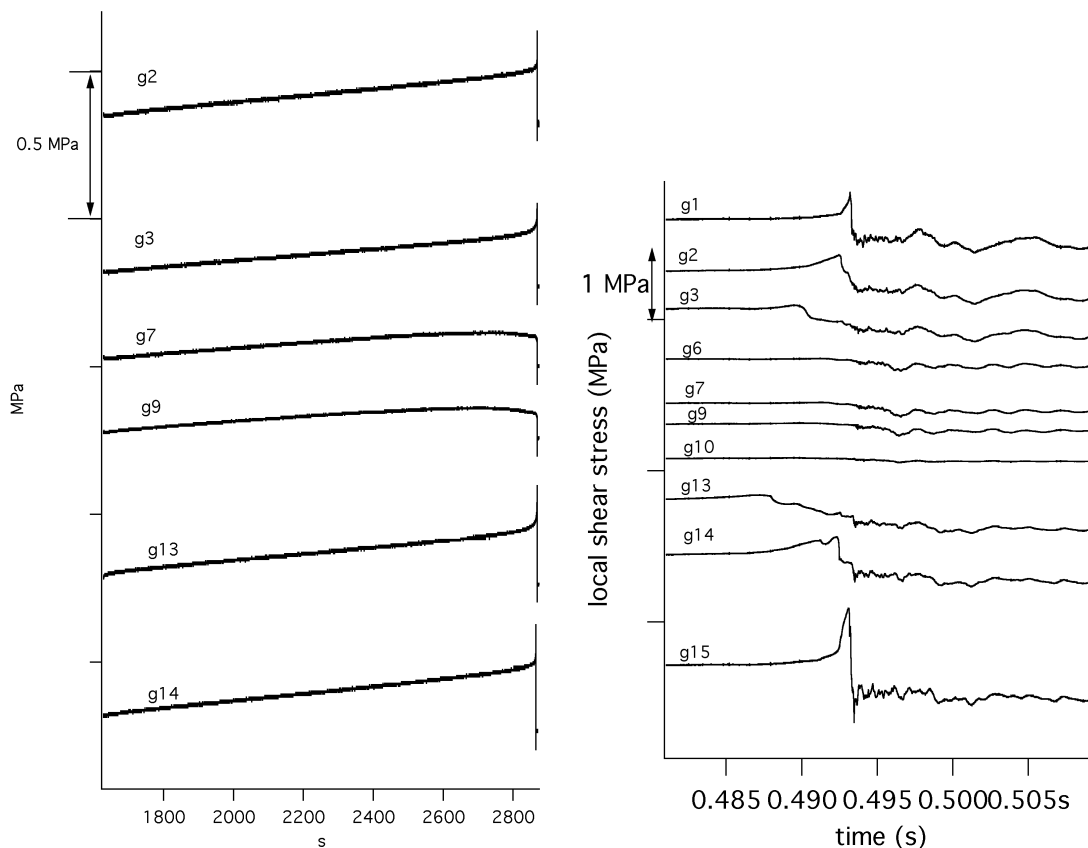


Figure 3 a) Long duration, low speed recording of loading, nucleation and stress drop. Shown are 6 stress records from positions along the fault surface. Records are offset vertically to reflect the spatial position of the instrument. Stress records show that the center of the fault undergoes precursory slip, dropping the fault strength in that region prior to the earthquake. Whereas, the ends experience stress transfer from the fault center, prior to the earthquake. b) Short duration, high speed recording of dynamic rupture for the event shown in Figure 3a. Shown are 10 stress records from the same 6 positions along the fault surface in shown in 3a and 4 additional instruments. Records are offset vertically to reflect the spatial position of the instrument.

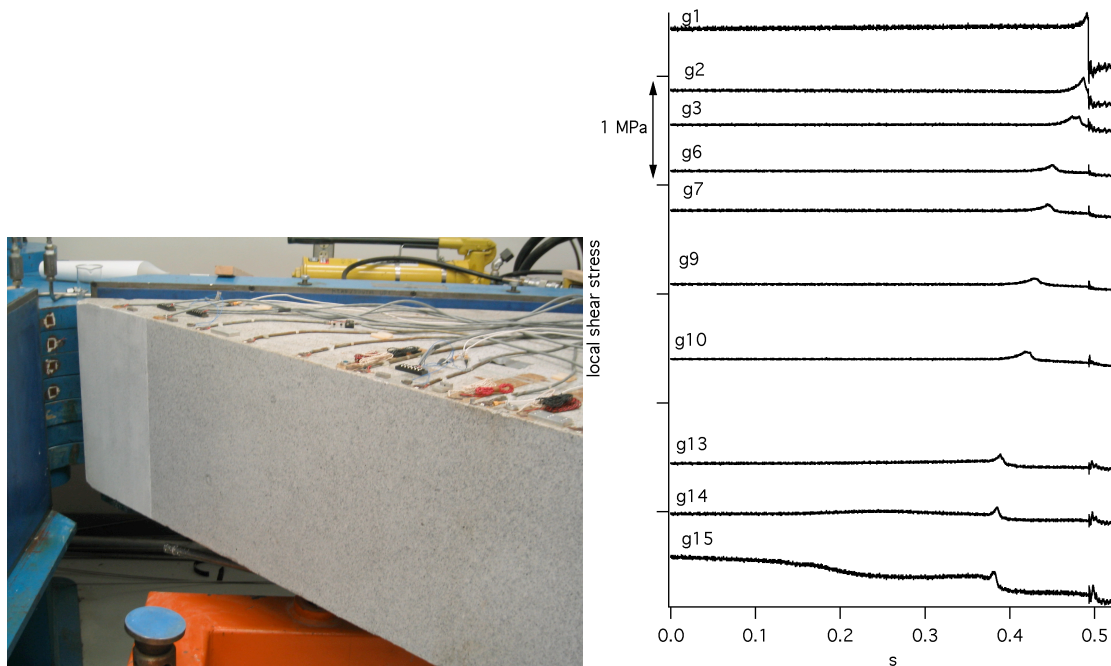


Figure 4. a) Simple heterogeneous fault consisting of bare Sierra granite with a thin layer of ultra-fine quartz powder at one end. b) High speed record of complex rupture for comparison with Figure 3b. Rupture is preceded by fault creep at one end (g15). Slow earthquake rupture nucleates at that end and propagates the entire length of the sample as evident from the stress pulse starting at g15 around 0.375 s and eventually reaching the opposite end (g1) just prior to 0.5 s. Dynamic earthquake rupture then propagates rapidly back down the fault from g1 to g15.

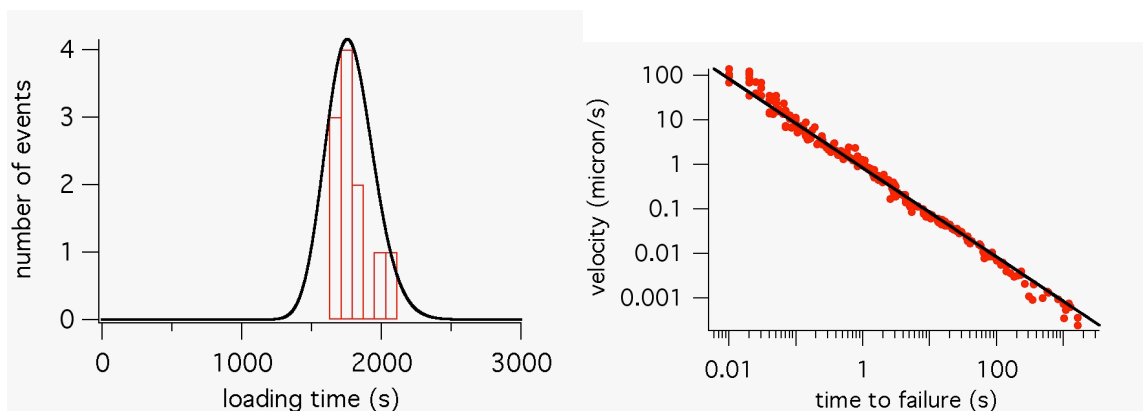


Figure 5. a) Histogram of loading time for 10 recurrences. Shown for comparison is a log normal distribution with mean 1770s and standard deviation of 170s b) Precursory slip rate prior to failure within the nucleation zone from the 11 events shown in Figure 5. This precursory slip is measured directly on the fault, in this case from cantilever slip gage c3 (see Figure 1) located near the fault center. The line is a fit with slope constrained to be -1 as predicted by Dieterich and Kilore (1996).